Peer reviewed version

Link to published version (if available):
10.1021/acs.molpharmaceut.6b01008

Link to publication record in Explore Bristol Research
PDF-document

University of Bristol - Explore Bristol Research
General rights

Functionalised triblock copolymer vectors for the treatment of acute lymphoblastic leukaemia

Robert C. Deller,[+] Paraskevi Diamanti,[+,§] Gabriella Morrison,[+] James Reilly,[+] Benjamin Ede,[+] Robert Richardson,[∥] Kristian Le Vay,[‡,†] Andrew M. Collins,[∥,†] Allison Blair*[,+,§,] Adam W. Perriman,*[,+ 1]

[+]School of Cellular and Molecular Medicine, University of Bristol, Bristol, UK.

[§]Bristol Institute for Transfusion Sciences, NHS Blood and Transplant, Bristol, UK.

[∥]School of Physics, University of Bristol, Bristol, UK.

[‡]School of Biochemistry, University of Bristol, Bristol, UK.

[†]Bristol Centre for Functional Nanomaterials, University of Bristol, Bristol, UK.

KEYWORDS

Pluronic, Poloxamer, Micelle, Parthenolide, Nanoparticle, Acute Lymphoblastic Leukaemia (ALL)

---

[1] *Corresponding Authors: Dr. Adam W. Perriman, chawp@bristol.ac.uk, +44 (0) 1173312140, Dr. Allison Blair, Allison.Blair@bristol.ac.uk, +44 (0) 1173312086

ABSTRACT

The chemotherapeutic Parthenolide is an exciting new candidate for the treatment of acute lymphoblastic leukaemia but like many other small molecule drugs, has low aqueous solubility. As a consequence, Parthenolide can only be administered clinically in the presence of harmful co-solvents. Accordingly, we describe the synthesis, characterisation and testing of a range of biocompatible triblock copolymer micelles as particle-based delivery vectors for the hydrophobic drug Parthenolide. The drug-loaded particles are produced via an emulsion-to-micelle transition method and the effects of introducing anionic and cationic surface charges on stability, drug sequestration, biocompatibility and efficacy are investigated. Significantly, we demonstrate high levels of efficacy in the organic solvent free systems against human mesenchymal stem cells and primary T-acute lymphoblastic leukaemia patient cells, highlighting the effectiveness of the delivery vectors for the treatment of acute lymphoblastic leukaemia.

INTRODUCTION

Many therapeutics exhibit high efficacy but suffer from low aqueous solubility, which limits their application as effective treatments.[1] Numerous strategies exist in order to improve the formulation and subsequent administration of such compounds, including the incorporation of organic co-solvents, production of synthetic analogues with greater hydrophilicity or use of prodrug precursors[2]. Unfortunately, the addition of organic co-solvents often results in adverse cytotoxic effects, severely limiting their clinical use. Furthermore, chemical modifications to introduce greater hydrophilicity not only require additional synthetic steps, but can also reduce drug efficacy. As a consequence, the application of polymer based micelles, vesicles and nanoparticles as drug delivery vectors is increasing substantially.[3] The attractiveness of polymer-based systems begins with their high degree of inherent tunability, for example, polymeric systems can be designed to respond to external stimuli such as temperature, pH or light allowing a controlled release profile.[4-6] Moreover, the incorporation of specific functional groups on the vector provides a robust route to biomolecule conjugation[7] or surface charged modifications to generate neutral, anionic, cationic or zwitterionic species, which can both aid in the targeting of specific cell populations to limit systemic exposure.[8-11]

Acute lymphoblastic leukaemia (ALL) is a disease with an incidence of 1 - 4.75 per 100,000 people globally[12], but with a much higher incidence in children, peaking at between 2 and 5 years of age.[13-15] With current treatment protocols, around 90% of childhood ALL achieve clinical remission.[16-18] However, approximately 20% of children relapse due to the persistence and continued proliferation of leukaemia cells that are resistant to therapy and many cases who relapse do not survive.[19] Treatment itself is extremely toxic and can be life threatening.[20] The lack of an effective, less toxic treatment programme has driven the requirement for alternative chemotherapeutic treatments and delivery mechanisms with several candidates as attractive targets including the drug Parthenolide (PTL).[1,21] PTL

3

(**Figure 1A**) is a natural product (sesquiterpene lactone) derived from *Tanacetum parthenium* (also known as feverfew) that has been shown to have excellent chemotherapeutic potential in the treatment of AML, and more recently ALL, but has an inherently poor aqueous solubility limiting bioavailability.[19,22,23] Though several studies investigating the use of a PTL (dimethylamino) analogue with improved aqueous solubility have been reported, its effectiveness as anti-proliferative agents is less pronounced and requires additional synthetic steps. A number of other analogues have also been recently reported, but also have reduced efficacy and at present are not suitable alternatives.[24,25]

Pluronics (also known as poloxamers) are a class of triblock copolymers of poly(ethylene) glycol (PEG) and poly(propylene) glycol (PPG) in the configuration PEG-PPG-PEG, and their complex mesophase behaviour makes them excellent candidates as drug delivery vectors.[26] For example, variations in the PEG (hydrophilic) and PPG (hydrophobic) compositions elicit notable differences in their critical micelle concentration (CMC) and critical micelle temperature (CMT).[27-29] This versatility has led to the application of Pluronic nanocarriers as vectors for drug delivery, as the hydrophobic PPG core provides an environment for compounds with poor aqueous solubility to be sequestered.[29,30] Notable examples include the use of folic acid functionalised P123/F127 mixed nanocarriers for paclitaxel delivery in multidrug resistant tumours and thermally responsive F127-chitosan nanocarriers for the intracellular delivery of small molecules.[31-33] Significantly, cationic F127-PEI conjugates have been shown to improve both the delivery of the anti-cancer compound docetaxel and a plasmid encoding the serine protease inhibitor TFPI-2.[34] These examples highlight the adaptability of Pluronic nanocarrier systems functionalised with small molecules, proteins or polymers as drug or gene delivery vectors.
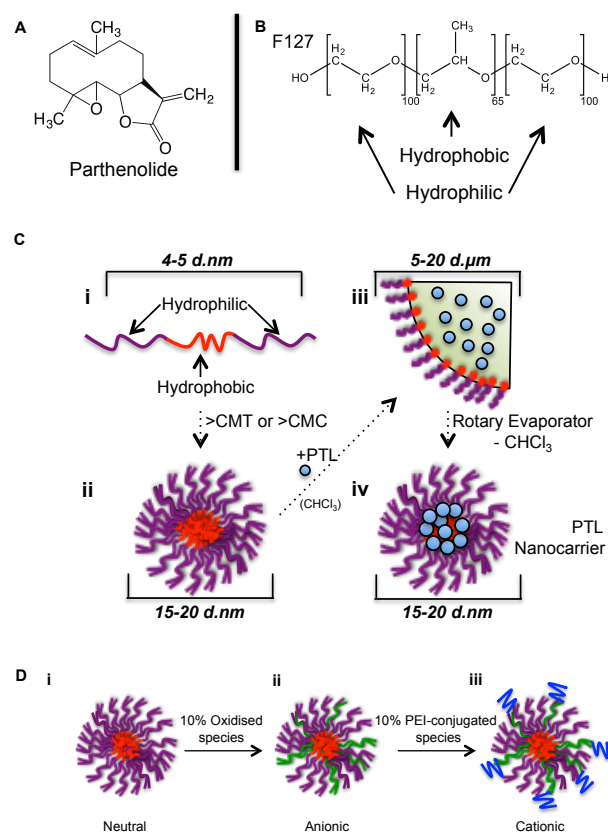
Figure 1: A. The structure of the chemotherapeutic parthenolide. **B.** Triblock co-polymer structure of Pluronic F127. **C.** Scheme highlighting the synthetic strategy to parthenolide loaded micelle formation. **i.** Monomeric F127 **ii.** F127 Micelle formation above CMT or CMC. **iii.** Addition of $CHCl_3$ and PTL forming a stable emulsion by vortexing. **iv.** Rotary evaporation to remove $CHCl_3$ and encapsulate PTL in solvent-free micelles. **D.** Micelle systems **i.** Neutral **ii.** Anionic (oxidised) **iii.** Cationic (PEI-conjugated).

In this study, we have produced a range of Pluronic micellar structures as vectors for the solvent free delivery of PTL for the treatment of ALL. Significantly, we demonstrate that PTL loaded F127 micelles could be used as an alternative for co-solvent PTL delivery to primary T-ALL cells. Furthermore, drug efficacy was varied between micelles displaying cationic charges compared to anionic formulations, emphasizing how charge can influence membrane interactions and subsequent drug delivery.

EXPERIMENTAL

Reagents

Parthenolide was purchased from Santa Cruz Biotechnology Inc. (Heidelberg, Germany) and of the highest available purity. All other reagents unless otherwise specified were purchased from either Sigma Aldrich Company Ltd (Poole, UK) or Life Technologies Ltd (Paisley, UK) and used without further modification.

Donor cells

Bone marrow samples were obtained with consent from healthy donors from whom mesenchymal stem cells were isolated in full accordance with Bristol Southmead Hospital Research Ethics Committee guidelines (reference #078/01). Bone marrow derived diagnostic primary T-ALL samples were collected, with consent, approved by University Hospitals Bristol Trust, Bristol, UK (REC 12/LO/1193). Primary T-ALL cells were isolated via ficoll mediated density gradient centrifugation and cryopreserved in vapour phase N_2 prior to use.

PTL loaded micelle synthesis

Parthenolide loaded micelles were synthesised using a modified strategy devised by Collins *et al* as PTL in an aqueous 10 wt % F127 solution alone does not enable effective partitioning into the micelles even with significant agitation.[30] In brief 12 mg of Parthenolide dissolved in 1 mL of chloroform is added to a 20mL aqueous 10 wt % Pluronic solution (all variations) at room temperature. The mixture is vortexed vigorously to ensure a stable homogeneous emulsion and partition of Parthenolide into the organic (chloroform) phase. The mixture is placed on a rotary evaporator (BUCHI UK Ltd, Manchester, UK) at 42 °C and 150 mbar for 60 minutes causing evaporation and elimination of

chloroform leaving (2.4 mM / 0.6 mgml^{-1}) Parthenolide loaded Pluronic micelles free from organic solvents for further use.

<u>*DPH assay (CMC and CMT)*</u>

1,6-diphenyl-1,3,5-hexatriene (DPH) displays a dramatic shift in fluorescence intensity when in a hydrophobic environment and is therefore an excellent probe for micelle formation. CMC can therefore be defined as follows: 200 μL of Pluronic (0 wt% - 5 wt%) is aliquoted in triplicate in a 96-well plate to which 10 μL DPH (saturated) in MeOH is added. Samples were placed on a rotator at 120 rpm for 10 minutes to ensure a homogenous suspension prior to measuring fluorescence (excitation 355 nm, emission 488 nm) using a Mithras LB 940 plate reader (Berthold Technologies GmbH & Co. KG, Bad Wildbad, Germany) with dramatic increases in fluorescence indicative of micelle formation. CMT was measured using a temperature controlled (Quantum Northwest Inc, Washington, USA) UV-Vis Spectrophotometer (Agilent Technologies LDA UK Limited, Stockport, UK). 400 μL of 2 wt% Pluronic plus 20 μL DPH (saturated) in MeOH was mixed and transferred to a quartz cuvette (1 cm pathlength) and absorbance measured continuously at 360nm from 6 °C to 40 °C at 1°C/min with a rapid increase in absorbance indicative of the onset of micelle formation.

<u>*Dynamic light scattering, Static light scattering and Zeta Potentiometry*</u>

All dynamic light scattering (DLS), static light scattering (SLS) and zeta potential measurements were performed using a Malvern Nano ZSP zetasizer (Malvern Instruments Ltd, UK) with samples filtered (0.22 μm) to remove large aggregates and contaminants immediately prior to analysis. Monomer size (DLS) and M_W (SLS) were defined at a concentration and temperature (4 or 25 °C) combination below the CMC and CMT. Micelle size (DLS) and M_W (SLS) were defined at a concentration and temperature (37 or 50 °C) combination above the CMC and CMT with minimum

equilibration time of 10 minutes. CMT measurements were performed at 1°C intervals at a concentration of 1 wt % (10 minute equilibration) from 4 – 40 °C with the onset of well-defined micelles indicative of the CMT. When highlighting the retention of PTL with respect to thermal reversibility temperatures of 4 and 42 °C were used with 10 wt% F127 micelles loaded with 0.6 mg.mL^{-1} PTL. Each of the reported values were performed in pure H_2O solutions.

Small Angle X-ray Scattering

Small Angle X-ray Scattering (SAXS) was measured using a GANESHA SAXS instrument (SAXSLAB, Denmark). The X-ray wavelength was 1.5 Å (copper Kα radiation), and scattering was detected using a Pilatus 300K 20Hz detector (Dectris AG Switzerland) giving a q-range of 0.01 – 0.3 Å^{-1} with measurements performed under vacuum. Samples were prepared to a final concentration of 2 wt% F127 ± 0.12 mg mL^{-1} (483 μM) PTL (a 5-fold dilution from the prepared stock in order to avoid the onset of a strong structure factor contribution from particle-particle interactions) in deionised water and sealed in quartz capillaries (SAXSLAB, Switzerland). Temperature was controlled using a Julabo temperature controller (Julabo GmbH, Germany) with a thermocouple within the sample chamber ensuring that an accurate and constant temperature was attained. Water and empty cell backgrounds were subtracted from the sample measurements. The radius of gyration and I(0) were obtained from the reciprocal and real space data using GNOM. Form factor fitting was performed in IGOR using a model form factor describing a population of spheres with uniform scattering length density (PolyRectSpheres, NCNR SANS analysis macro). A spherical model was chosen rather than a core shell model as the difference in contrast between phases was not sufficient to be distinguished using a benchtop instrument. The *scale* parameter, corresponding to the volume fraction of F127, was fixed at 0.018, the *background* parameter was then fitted and subsequently fixed. *Polydispersity* and *solvent scattering length density* (*SLD*) were held at 0.01 and 9.43E-6 Å^{-2} respectively. The data were then

fitted, floating the *radius* and *sphere SLD* parameters. The micelle aggregation number was calculated by first determining f, the ratio of F127 to water in the micelle (**Equation 1**).

Equation 1.
$$f = \frac{I(0)}{\varphi_{micelles} \cdot V_{micelle} \cdot (SLD_{F127} - SLD_{H_2O})^2}$$

Where f is the volume fraction of F127 in the micelle, $\phi_{micelles}$ is the volume fraction of micelles in the sample, $V_{micelle}$ is the micelle volume, calculated from the form factor fit radius, and I(0) is the extrapolated scattering intensity at zero-angle, determined from the real space transformation of the data. SLD values were calculated by summing scattering length contributions over all atoms per molecule and dividing by the molecular volume. The volume of F127 per micelle was then calculated and divided by the molecular volume to give the aggregation number. The molecular volume of F127 was previously determined by Bogomolova *et al*. (2013).[35]

Synthesis of RITC labelled F127

Rhodamine B isothiocyanate (RITC) was conjugated to F127 via the terminal hydroxyl groups. RITC (1 mg.mL^{-1}) was added to 10 wt% solution of F127 in DMSO and stirred at room temperature in the dark for a minimum of 48 hours to enable conjugation. Preparations were then subsequently dialysed against 5L H_2O with a MWCO of 3.5kDa and subjected to a minimum of three H_2O changes in order to liberate any unbound dye. The F127-RITC conjugates were then freeze-dried to yield a solid preparation for further use. Conjugation efficiency was verified using UV-Vis spectroscopy, and micelle formulations were prepared with low concentrations of RITC-F127 in order to eliminate influences of the dye molecules on micelle formation, uptake and cytotoxicity.

Synthesis of carboxylic acid terminated (anionic) F127

A 10 wt% solution of F127 in H_2O equating to 5g of F127 was prepared to which 175 mg sodium bromide, 75 mg 2,2,6,6,-tetramethyl-1-piperidinyloxyl (TEMPO) and 15 mL sodium hypochlorite solution containing 10-15 % available chlorine were added with the resulting mixture adjusted to pH11. The solution was left stirring overnight at room temperature with periodical pH adjustments upwards to pH11. Afterwards, the solution was quenched with 25 mL of ethanol and the reaction adjusted to pH1 prior to solvent extraction with 3x100mL aliquots of chloroform. The organic fractions were subsequently washed with 3x100mL aliquots of H_2O (pH1) prior to rotary evaporation at 42 °C and 150 mbar for 60 minutes. Upon cooling to room temperature the resulting solid was dissolved in ethanol at 60 °C and then left overnight at -20 °C to recrystallise. The chilled ethanol solution was then decanted and the oxidised F127 product dried further using a rotary evaporator to remove residual ethanol.

Synthesis of PEI labelled (cationic) F127

Poly(ethylenimine) (PEI) with an average M_w of 1.3 kDa was conjugated to oxidised F127 mediated by EDC.[36] In brief 100 μL of 50% (v/v) PEI in H_2O was mixed with 2 mL of 10 wt% (10% oxidised) F127 in H_2O to which 33 mg of EDC (1-ethyl-3-(3-dimethylaminopropyl)carbodiimide hydrochloride) and 40 mg NHS (N-Hydroxysuccinimide) is added and adjusted to pH 4 for a minimum of 24 hours. Preparations were then subsequently dialysed against 5L H_2O with a MWCO of 3.5kDa and subjected to a minimum of three H_2O changes in order to liberate any unbound PEI. The F127-PEI conjugate was then freeze-dried to yield a solid preparation for further use.

Microscopy

Widefield microscopy was performed using a Leica DMI6000 inverted epifluorescence microscope coupled with a Leica DFC365FX monochrome CCD camera in a temperature (37 °C) controlled environment equipped with a range of 5x to 100x dry/oil objectives. Confocal microscopy was performed using a Leica SP8 AOBS confocal laser scanning microscope attached to a Leica DM I6000 inverted epifluorescence microscope with 'Adaptive Focus Control' in a temperature (37 °C) controlled environment with a range of 10x to 100x dry/oil objectives.

Assessment of Pluronic F127 cytotoxicity on hMSCs

Human mesenchymal stem cells (hMSCs) (passage 3) were cultured in a 96-well plate until confluent in hMSC medium (DMEM (low glucose), 10% (v/v) FBS, 2mM Glutamax, 100 units/mL Penicillin and 100 μg/mL Streptomycin). Each well was then replaced with 160 μL hMSC media plus 40 μL pre-prepared F127 micelles (0 - 10 wt%) with 4 replicates and incubated at 37 °C / 5% CO_2 for 18 hours yielding a final concentration of Pluronic F127 between 0 – 2 wt%. Cells were washed with 200 μL PBS prior to metabolic activity assessment by established Alamar Blue assays.

In vitro drug sensitivity with hMSCs

hMSCs (passage 2) were placed in 96-well plates in hMSC media until confluent. Cells were incubated with 160 μL hMSC media plus 40 μL pre-prepared F127/PTL micelles (0 wt% - 2.5 wt% F127) or 40 μL PTL co-solvent (2.5% methanol (v/v)) with a final PTL concentration varying from 0 μM – 10 μM and 0.5 wt% F127 (n=4). Cells were then incubated at 37 °C / 5% CO_2 for 24 hours and washed with 100 μL PBS prior to metabolic activity assessment by established Alamar Blue (24 hours) assays.

In vitro drug sensitivity with T-ALL cells

Cryopreserved primary T-ALL cells were thawed and initial cell viability (> 60%) measured by flow cytometry using propidium iodide (PI)(Miltenyi Biotec Ltd, Bisley, UK). Cells were plated as 160 μL aliquots in triplicate in a round-bottom 96 well plate ($4x10^4$ live cells per well) in RPMI 1640 supplemented with 25% (v/v) FBS, 2mM Glutamax, 100 units/mL Penicillin and 100 μg/mL Streptomycin prior to the addition of 40 μL of the corresponding F127 preparation and incubated at 37 °C / 5% CO_2 / 5% O_2 for 24 hours. Cells were then centrifuged at 500g for 5 minutes at room temperature and the supernatant discarded. Cells were resuspended in 100 μL of 2.5 %(v/v) Annexin-V solution (Miltenyi Biotec Ltd) and incubated in the dark at room temperature for 10 minutes. Afterwards 100 μL of Annexin-V buffer was added prior to a second wash step. The supernatant was discarded and cells resuspended in 100 μL of Annexin-V buffer and cooled to 4°C prior to analysis. Analysis was performed on a MACSQuant® Analyser 10 flow cytometry (Miltenyi Biotec Ltd) with the pre-addition and mixing of PI to allow differentiation between necrosis and apoptosis. The resulting data was analysed using FlowJo single cell analysis software (FlowJo LLC, OR, USA) gated for the selection of lymphocytes and further gated to into quadrants comprising live, early apoptotic, late apoptotic and dead cells (Supplementary Figure. 15). Viabilities are expressed as a percentage of untreated controls.

LogP and Volume Calculations and Statistics

Theoretical calculations to determine LogP and (van der Waals) surface area values of F127, PTL, and DPH were derived using MarvinSketch 16.1.25.0 (release date 2016) accessible at http://www.chemaxon.com. Data interpretation, numerical and statistical analysis were performed using Microsoft® Excel® for Mac 2011 (Microsoft Corporation, WA, USA), Origin 9.0 (Originlab

Corporation, MA, USA) and Prism 7 for Mac OS X (Graph Pad Inc, CA, USA). IC_{50} values were defined using a sigmoidal dose response algorithm.

Mass spectrometry (MALDI-TOF).

Matrix assisted laser desorption ionisation time of flight (MALDI-TOF) mass spectrometry was performed on a UltrafleXtreme mass spectrometer (Bruker (UK) Ltd, Coventry, UK) using a matrix of containing a saturated solution of α-Cyano-4-hydroxycinnamic acid in acetonitrile with 0.1% trifluoroacetic acid in an 1:1 ratio of sample in H_2O mixed and spotted onto a 384 well plate with a ground steel surface prior to ionisation and detection (100% laser power / +ve ion mode. Analysis was performed using the open source software mMass (v. 5.5)[37] accessible at http://www.mmass.org/.

Fourier transform infrared spectroscopy (FTIR).

FTIR spectroscopy was performed on a Spectrum One Fourier Transform Infra‑ Red (FTIR) spectrometer equipped with a universal attenuated total reflectance (ATR) sampling accessory (Perkin Elmer Inc, MA, USA). Small quantities of solid Pluronic and the oxidised and PEI analogues were separately placed over the quartz window and the sample tightened to ensure accurate measurement. A total of 8 replicates were performed and the averages were reported. The appearance of a carbonyl stretching vibration at 1740 cm^{-1} was indicative of successful oxidation and presence of a (anionic) carboxylic acid functional group. The appearance of an amine bond stretching vibration at 3410 cm^{-1} was indicative of successful coupling and the presence of (cationic) amine functional groups derived from PEI. For chloroform detection small quantities of the appropriate F127 solution/emulsion was placed over the quartz window and the sample tightened to ensure accurate measurement. A total of 20 replicates were performed and the averages were reported. The presence of chloroform could be monitored by the appearance of a carbon-chlorine stretching vibration at approximately 750 cm^{-1}.

RESULTS AND DISCUSSION

Properties of F127 micelles.

Pluronic molecules undergo a reversible monomer/micelle transition that is dependent upon both temperature (CMC) and concentration (CMT) and it was essential to understand this behaviour for effective vector design (**Table 1**).[26] The Pluronic molecule (**Figure 1B**) F127 (Poloxamer 407) was selected as it is widely available and FDA approved as a pharmaceutical ingredient and foodstuff.[33,38] MALDI-TOF mass spectrometry from the F127 gave a mass of 13.5 ± 0.8 kDa (FWHM), which was close to the theoretical value of 12.6 kDa (**Supplementary Figure 1**). Discrepancies between MALDI-TOF mass spectrometry and the theoretical value can be explained in part due to shifts in the polymer mass distribution often associated with this technique.[39] F127 and acid- or poly(ethylenimine)-modified analogues (see *Materials and Methods* for the synthesis of carboxylic acid terminated and PEI labelled F127) were used to produce PTL loaded micelles (**Figure 1C**) with neutral, anionic or cationic peripheral surface charges respectively (**Figure 1D**).

Table 1: Properties of F127 with respect to size, phase and aggregation number.

Property	F127
Monomeric hydrodynamic diameter (DLS)	3.4 ± 0.2 nm (5 wt% / 4 °C) (PDI; 0.254 at 10°C)
Micelle hydrodynamic diameter (DLS)	20.2 ± 0.3 nm (5 wt% / 37 °C) (PDI; 0.048 at 37 °C)
Micelle diameter (SAXS)	19.2 ± 2.2 nm (2 wt% / 31 °C)
	20.0 ± 2.0 nm (2 wt% / 37 °C)
	20.7 ± 1.9 nm (2 wt% / 49 °C)
CMT (DPH)	25 ± 1°C (2 wt%)
CMT (DLS)	25 ± 1°C (1 wt%)
CMC (DPH)	1.5 ± 0.25 wt% (25 °C)
Aggregation No. (SLS)	40 ± 2 (50 °C)
Aggregation No. (SAXS)	46 ± 2 (37 °C)
Mass (MALDI-TOF)	13.5 ± 0.8 kDa

* DLS - dynamic light scattering

† SAXS - small angle x-ray scattering

†† DPH - 1,6-diphenyl-1,3,5-hexatriene (DPH) assay.
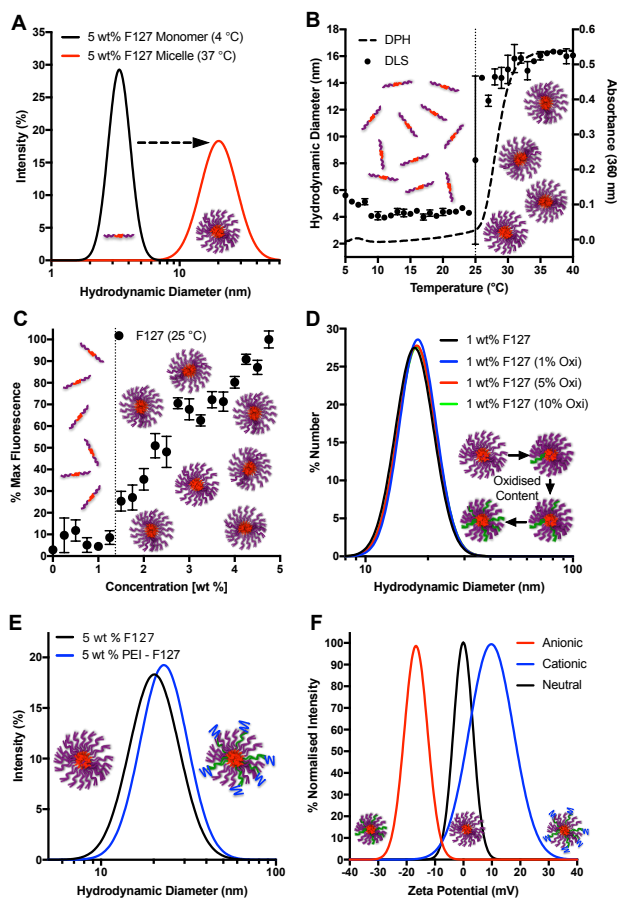
** SLS – static light scattering

Dynamic light scattering (DLS) measurements of 5 wt% aqueous solutions of F127 at 4 and 37 °C gave hydrodynamic diameters 3.4 ± 0.2 nm and 20.2 ± 0.3 nm for the monomeric and micelle phases of unmodified F127 respectively (**Figure 2A**). Monitoring changes in hydrodynamic diameter with respect to temperature allowed the determination of the CMT ($25 \pm 1°C$) (**Figure 2B**). This was complemented by an absorbance/fluorescence based micellization assay utilising the hydrophobic dye 1,6-diphenyl-1,3,5-hexatriene (DPH), which gave a CMT value of $25 \pm 1°C$. Here, upon micelle formation and the subsequent sequestration of DPH into the hydrophobic core, a considerable change in the fluorescence depolarization of DPH causes a substantial increase in absorbance and fluorescence enabling the onset of micelle formation to be identified with respect to both the CMT and CMC (**Figure 2B & Figure 2C**).[40] An aggregation number of 40 ± 2 was evaluated by SLS using previously reported refractive index increment values for F127 at 25 °C and 50 °C with a comparable value of 46 ± 2 (37 °C) determined by SAXS (**Supplementary Figure 2 & Supplementary Table 1**).[41] This was crucial in estimating the micelle number density, number of PTL molecules per micelle and average peripheral surface charge. The aggregation number is known to increase with temperature although with no observed increase in hydrodynamic diameter *via* DLS, which has been shown in part to be due to the H_2O hydration of the PEO blocks.[42,43] Accordingly, temperature-dependent small angle x-ray scattering (SAXS) experiments were used to probe changes in micelle diameter with respect to temperature, which showed a 1.5 nm increase in the particle radius as the temperature was increased from 31 to 49 °C (**Supplementary Figure 3 & Table 1**).

Incorporation of anionic and cationic peripheral surface charge.

The inclusion of peripheral surface charges can begin to introduce elements of specificity and targeting as well as expanding chemical functionality for further modification. In order to initiate a peripheral anionic surface charge, the terminal hydroxyl groups of F127 were quantitatively oxidised to

yield carboxylic acid functional groups. Effective oxidation was confirmed by Fourier Transform Infrared (FTIR) spectroscopy with the appearance of a peak at 1740 cm^{-1}, indicative of a carbonyl (C=O) stretch (**Supplementary Figure 4**).

Figure 2: Characterisation of F127 Micelles **A.** Dynamic light scattering of F127 below and above the CMC and CMT highlighting the hydrodynamic radius of the monomeric and micelle species. **B.** CMT evaluation of F127 by DLS (1 wt%) and the DPH (2 wt%) assay. **C.** CMC evaluation of F127 by the DPH assay at 25 °C. **D.** DLS of 1 wt% F127 micelles with a range of oxidised substituents (0-10%) in PBS at 37 °C. **E.** DLS of 1 wt% F127 micelles conjugated with PEI in PBS at 37 °C. **F.** Zeta potential of F127 (neutral), Oxidised F127 (anionic) and PEI-F127 (cationic) at pH 7.1.

Preparations consisting of 100% oxidised F127 significantly reduced the cloud point transition temperature from in excess of 65 °C for unmodified F127 to 25 °C for a 100% oxidised preparation at 1 wt%, rendering the formulation unusable for vector design. However, creating a blend consisting of 50% oxidised F127 and 50% F127 did alleviate this effect (**Supplementary Figure 5**). As the oxidised content was increased from 0 to 10%, a reduction in DPH fluorescence was also observed (**Supplementary Figure 6**) without a significant change (p-value >0.05) in the hydrodynamic diameter of the corresponding micelles (**Figure 2D & Table 2**).

A reduction in DPH fluorescence was consistent with an increase in the dielectric constant of the micelles arising from the charged headgroups. Therefore, micelles with an oxidised content equating to 10% (average of 4 oxidised monomers per micelle) were taken forward for subsequent *in vitro* experiments. For cationic particle synthesis, poly(ethylenimine) (PEI) ($\approx$ 1.3 kDa) was coupled to the oxidised F127 adduct and efficient coupling was verified by the presence (3410 cm^{-1}) of N-H stretching vibrations in the resulting FTIR spectra (**Supplementary Figure 4**). DLS experiments performed on the PEI conjugated cationic micelles (10% PEI content) showed a 2 nm increase (p-value <0.0001) in hydrodynamic diameter when compared with the pristine particles (**Figure 2E, Table 2**), although no increase in radius was observed by SAXS, which was consistent with a diffuse low contrast PEI corona with aggregation number (SAXS) values comparable to the pristine particles (**Table2, Supplementary Table 2 and Supplementary Table 3)**

Table 2: Properties of oxidised F127 and PEI conjugated F127 with respect to micelle size and aggregation number at various levels of oxidised or PEI content. Values represent the mean ± standard error.

Property	Oxidised F127	PEI-F127
Micelle hydrodynamic diameter (DLS)	20.2 ± 0.3 nm (0% /5 wt%) 17.2 ± 0.3 nm (0% /1 wt%) 17.9 ± 0.3 nm (1% /1 wt%) 17.7 ± 0.3 nm (5% /1 wt%) 17.7 ± 0.3 nm (10% /1 wt%)	22.9 ± 0.3 nm (10% /5 wt%)
Micelle diameter (SAXS)	20.1 ± 0.1 nm (10% /2 wt%)	20.0 ± 0.1 nm (10% /2 wt%)
Aggregation No. (SAXS)	45 ± 2 (10% /2 wt%; 37 °C)	43 ± 2 (10% /2 wt%; 37 °C)

* DLS - dynamic light scattering

† SAXS - small angle x-ray scattering

PEI and nanoparticles displaying PEI have been shown to have a high affinity for the anionic cell membrane surface and have been used as transfection agents for DNA delivery.[44,45] However, high M_W PEI cations can promote the aggregation/cross-linking of cells in suspension as well as being cytotoxic.[46-48] Therefore, it was postulated that low M_W PEI displaying F127 micelles may have a greater affinity for the cell membrane and further enhance solvent-free PTL uptake. To estimate the surface charge of each of the systems, zeta potentiometry was undertaken. Here, 2 mg.mL^{-1} micelle preparations at pH 7.1 (**Figure 2F**) gave zeta potentials of -16.5 ± 0.9 mV, +10.8 ±1.6 mV, and -3.2 ± 2.1 mV for the anionic, cationic and neutral particle systems, respectively.

Formulation of PTL loaded F127 micelles

Due to the insolubility of PTL in the aqueous phase and the toxicity of organic solvents the formation of PTL loaded F127 micelles (**Figure 1C**) was performed using a modified strategy derived from Collins *et al.* and was systematically applied across all three charged systems.[30] A notable difference in the synthesis was the implementation of a rotary evaporator step to eliminate chloroform as opposed to

microwaves, as rotary evaporation offers a greater degree of control and limits water loss. Here PTL ($\approx$20 mg.mL^{-1}) dissolved in chloroform (5% (v/v)) was used as the droplet phase in an oil-in-water emulsion, which was stabilised by the presence of the F127 (**Supplementary Figure 7 & Supplementary Figure 8**). The high log P value of PTL (3.07) ensured retention in the (hydrophobic) oil ($CHCl_3$) droplets. Complete removal of chloroform resulted in the collapse of the F127 stabilised emulsion droplets resulting in the formation of the PTL-loaded micellar structures. The removal of chloroform was confirmed by FTIR equipped with an ATR accessory and the elimination of a carbon-chloroform stretching vibration at 750 cm^{-1} (**Supplementary Figure 9**). The preparative mixtures (10 wt% F127, 2.42 mM PTL) yielded micelles with an average of 22 PTL molecules per particle and no large aggregates were detected, indicating complete PTL incorporation. The ability to systematically vary the concentration of PTL in F127 micelle systems was dependent upon a number of factors: the solubility of PTL in chloroform; the chloroform/aqueous F127 ratio for emulsion stabilisation; which in turn was dependent upon the concentration of ($\approx$10 %(v/v)) $CHCl_3$ in an aqueous 10 wt% F127 solution (**Supplementary Figure 10**)); and finally the maximum stable loading of PTL per micelle/F127 molecule. Estimation of the van der Waals volume of PTL indicated that the addition of PTL would only constitute an approximate 1% increase in the total micelle volume, which was consistent with DLS measurements that showed no appreciable changes in the particle hydrodynamic diameter. SAXS measurements also showed no significant increase in size for the pristine particles after the addition of PTL, but an increase in particle radius was observed for both the anionic and cationic micellar systems (**Supplementary Figure 11**), indicating a change in the packing density of the charged monomers arising from repulsive electrostatic headgroup interactions. Significantly, attempts to directly dissolve PTL into a concentrated micellar solution of F127 (>10 wt%) were unsuccessful, demonstrating the utility of the emulsion transfer methodology. Over the concentration range investigated, no PTL precipitate or significant change in size (*p*-value =0.9996) were detected (DLS) even after prolonged

exposure at 4 °C (below the CMT), which indicated that PTL (248 Da) could remain co-solvated by monomeric F127 (12.6 kDa) due to the low PTL:F127 (0.5:1) stoichiometry. Moreover, heating the sample back to 42 °C resulted in micelle formation with no significant (p-value = 0.9979) differences in the particle hydrodynamic diameters (**Supplementary Figure 12**). Complementary temperature-dependent SAXS experiments supported the DLS observations, showing no apparent change in the micelle diameter or PTL aggregate formation after a thermal cycle between 37 °C and 4 °C (**Supplementary Figure 13**). Significantly, increasing the PTL particle loading by an order of magnitude did result in visible PTL precipitate after storage (48 hour) at 4 °C. The ability to thermally cycle the system without the loss of sequestered PTL was significant, as retaining a consistent temperature above the CMT during an entire supply chain process of a therapeutic would be prohibitive. Moreover, low temperatures (e.g., 4 or -20 °C) are preferable to maintain sterility and prolong the shelf life of the active (drug) component.

Cell uptake and efficacy

Assessing the uptake and internalization and the resulting efficacy of PTL is critical for investigating the use of PTL loaded F127 micelles as a potential therapeutic. Bone marrow derived human mesenchymal stem cells (hMSCs) were assayed initially as they are well characterised and occupy a similar niche to lymphoblasts associated with ALL, though notable differences with respect to nanoparticle uptake and interaction may still exist.[49,50] Interactions between PTL-free rhodamine labelled F127 (biocompatible) micelles and hMSCs were studied using widefield fluorescence microscopy, which showed strong cell association after 15 minutes (**Supplementary Figure 14**). To probe the internalisation of F127, confocal fluorescence microscopy was utilised which showed F127 (red) in the cytoplasm but not in the nucleus (blue) (**Figure 3A** and **Figure 3B**), which was consistent with previously reported findings that utilised Nile Red as fluorescent hydrophobic probe in core cross-

linked poly(pentaerythritol tetraacrylate) stabilised F127 micelles.[51] It was not clear whether or not micelles or monomeric species persisted in the intracellular or membrane bilayer environment. Indeed, if PTL molecules were immobilised at the cytoplasmic membrane surface, it is possible that the drug would be internalised and progressed along its standardised chemotherapeutic pathway (e.g. NF-κB inhibition, p53 activation etc.), inducing apoptosis[20,22,24,52] by a mechanism similar to co-solvent administered PTL. However the internalisation of micelles or monomers (with associated PTL) and subsequent liberation of PTL cannot be ruled out.

To ensure that F127 micelles devoid of PTL but subjected to the same synthetic process (i.e. CHCl$_3$ addition and removal) did not incite cytotoxicity, hMSCs were incubated over a 18-hour period with subsequent cell metabolic activity (alamar blue)[53] measured. Even at the highest concentration tested (2 wt%) (**Figure 3C**), no cytotoxicity was observed, which is consistent with previous reports.[51,54] To investigate the intracellular delivery of PTL (72 μM), an initial qualitative evaluation by widefield microscopy of each F127 (1.5 wt%) charge type and co-solvent formulation was undertaken. The rapid (10 minutes) onset of toxicity indicated by changes in morphology and rounding (**Figure 3D, Figure 3E & Supplementary Figure 15**) showed qualitatively that PTL loaded F127 micelles still possessed an efficacious effect albeit at a concentration exceeding that of previous reported IC$_{50}$ values attained with other cell types.[21-25]
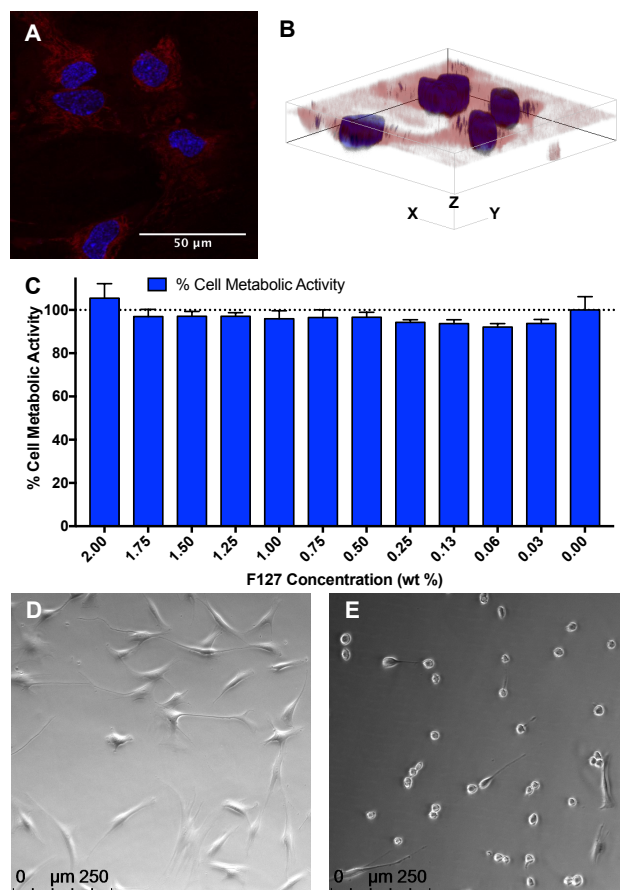
Figure 3: A. Confocal micrograph highlighting the retention of (PTL free) 2 wt% F127-RITC (red) and Hoechst 33342 (blue) after a 30 minute incubation with hMSCs cells. **B.** 3D projection of hMSCs highlighting distribution of F127-RITC (red) compared to Hoechst 33342 (blue). **C.** Relative cell metabolic activity (Alamar Blue) of hMSCs after an 18-hour exposure with various concentrations of unmodified Pluronic F127. Measurements are compared to an untreated control with the mean + standard deviation of at least 3 replicates reported. **D.** Micrograph of live hMSCs prior to administration of 72 μM PTL in 1.5 wt% F127 micelles. **E.** Micrograph of hMSCs treated with 72 μM PTL in 1.5 wt% F127 micelles after 45 minutes displaying significant altered morphology/rounding.

Leading on from this, quantitative dose response curves of each F127 micelle class (**Figure 1D**) were generated against hMSCs after an 18 hour incubation period (**Figure 4**) (allowing the onset of apoptosis), which revealed a reduction in cell metabolic activity (alamar blue) due to cell death, yielding IC_{50} values of 2.3 ± 0.2 μM, 2.8 ± 0.2 μM and 3.0 ± 0.2 μM for the cationic, neutral and

anionic preparations respectively. Differences between Pluronic and co-solvent ($IC_{50} = 1.8 \pm 0.1$ μM)

preparations were apparent, though evidently the use of F127 can substitute the need for co-solvent

(methanol) administration without a substantial loss of efficacy.
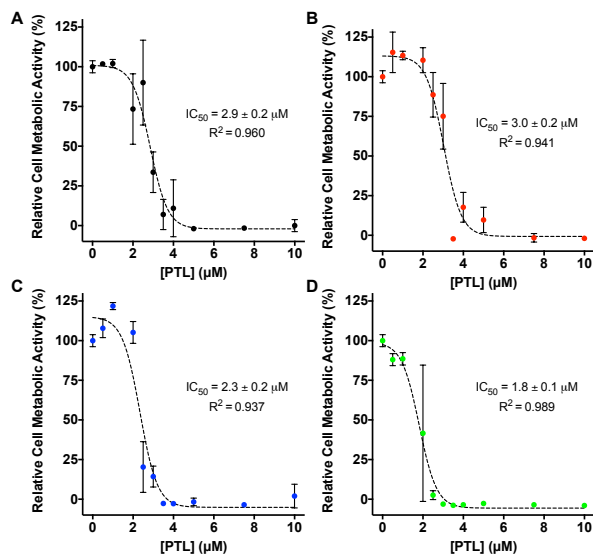
Figure 4: Dose response curves of various PTL formulations against hMSCs (passage 3) measuring

cell metabolic activity (alamar blue) relative to untreated controls. **A**. 0.5 wt% F127/PTL formulation.

B. 0.5 wt% 10% Oxidised F127/PTL formulation. **C**. 0.5 wt% PEI-F127/PTL formulation. **D**. Standard

(2.5% v/v) methanol/PTL co-solvent formulation. Values reported represent the mean of at least three

replicates and error bars ± standard deviation. IC_{50} values are derived from sigmoidal dose-response

curves with errors representing standard error.

Differences between each of the charged formulations may be rationalised by consideration of the

cell membrane surface charge. Specifically, the presence of predominantly anionic glycoproteins,

oligosaccharides and other elements of the glycocalyx generate regions of anionic surface charge,

which has been shown to detrimentally influence the interaction and uptake of nucleic acids and other

anionic constructs[55], which can be overcome by the introduction of cationic residues.[56-58] Therefore, it is

probable that the presence of cationic PEI promoted greater retention at the cell membrane resulting in

an increased probability of endocytosis when compared with the anionic or neutral particles. Indeed charge-mediated repulsion may explain the reduction in efficacy for the anionic system.

In light of the encouraging results from the hMSC assays, primary T-ALL cells were assessed as a more clinically relevant and direct measure of these F127 micelle preparations, especially as differences between the uptake of anionic and cationic nanoparticles between different cell types has been previously reported.[27-29,49,59] Previous endpoint (alamar blue) assays focused on the resulting cell metabolic activities of hMSCs, however, these assays do not discriminate between necrosis and apoptosis. Accordingly, an annexin-V/PI based flow cytometry assay[60] was implemented to differentiate between apoptotic and non viable (PI$^+$) populations and attribute apoptotic cell death caused by PTL (**Supplementary Figure 16**). Importantly no significant cytotoxicity was detected with a 2 wt% F127 (PTL free) solution with cell viability remaining close to untreated controls (96.4% ± 9.8%). Each F127 preparation induced apoptosis of T-ALL cells, with dose response curves reported (**Figure 5**) comparable to values in co-solvent administrated preparations, again highlighting the ability for co-solvent elimination. While, the variations arising from differences in charge were less clear, Patient A showed a reduction in efficacy in the anionic and cationic formulations, this was not apparent with Patient B and Patient C, with distinctions in patient response typical of the disease.[19] However, F127-PTL was most effective across the patient samples tested achieving higher levels of T-ALL cell killing using lower doses of drug (<2.4μM).

24
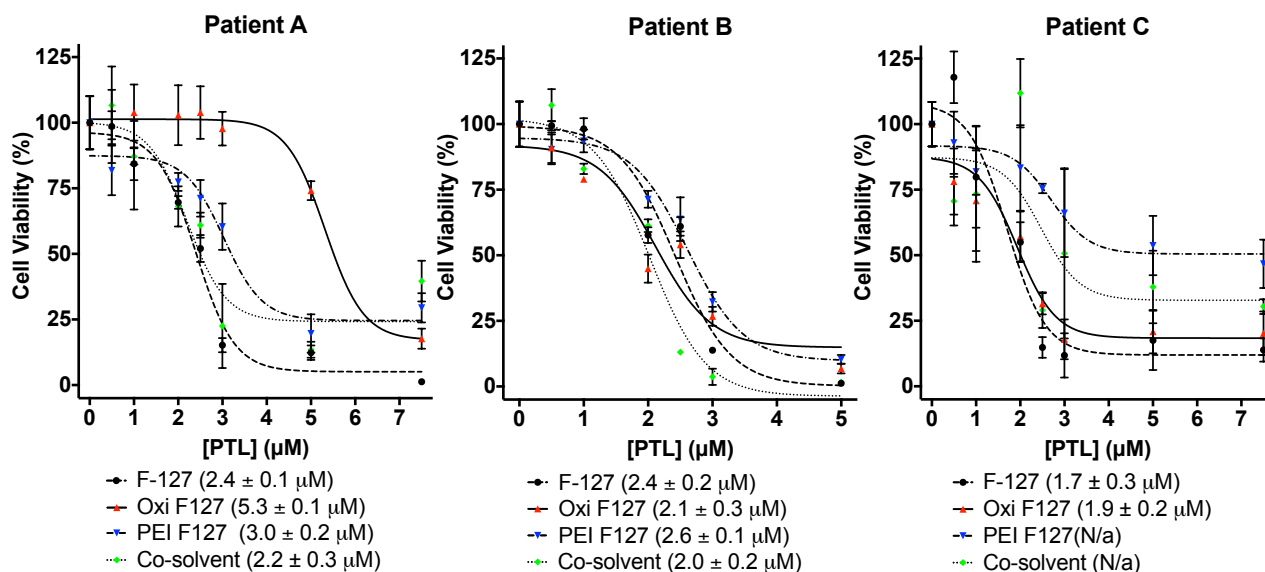
Figure 5: Dose response curves of all PTL formulations against patient T-ALL cells measuring apoptosis (Annexin V) and necrosis (propidium iodide) relative to untreated controls. **A.** Patient A. **B.** Patient B. **C.** Patient C. Values reported represent the mean of at least three replicates and error bars ± standard deviation. IC_{50} values are derived from sigmoidal dose-response curves with errors expressed as the standard error.

In these cases, the dose response associated between hMSCs and T-ALL cells did not differ dramatically such that no obvious therapeutic window could be derived, which further emphasises the importance of targeting/homing to limit systemic exposure. However, the utility and biocompatibility of using solvent-free formulations is highly attractive and another consideration is that *in vivo* dosimetry profiles of free (*i.e.* cytotoxic co-solvent) PTL tend to require multiple doses due to the relatively short half-life (<90 minutes in human liver microsomes), which could lead to an accumulation of the co-solvent.[61] Pluronic micelles have been reported to enhance the pharmacokinetic profile of the chemotherapeutic paclitaxel and therefore the use of F127 micelles may allow for a more infrequent and controlled dosimetry *in vivo*.[62] The effect of charge on micelles administered *in vivo* may also be more pronounced with respect to charge mediated attraction/repulsion, as the site of administration is often different (i.e. intravenous, intraperitoneal, oral etc.) to the desired treatment

locale. The effect of charge in a more biorelevant system may therefore be more pronounced with regards to distribution and persistence as seen with other polymer based micelle systems.[63]

Recent work has highlighted how in biological fluids both *in vitro* and *in vivo* a (plasma) protein corona often forms around nanoparticles that can influence their fate within living systems.[64,65] However, the extent of how this effect may impact pathophysiology is dependent on many factors, including the inherent nanoparticle composition and surface.[66,67] Surface modifications, such as the PEGylation of nanoparticles or drugs have been shown to limit (but not eliminate) protein adsorption. Indeed, protein adsorption to PEGylated surfaces appears to be necessary in order to prolong circulatory half-life and reduce non-specific cellular uptake, *i.e.*, the "stealth effect" could be a prerequisite for specific targeting strategies.[68-70] Similar mechanisms have been reported with Pluronic-based coatings in extending circulatory times[71-73] as well as with a range of amphiphilic block co-polymer micelles akin to those used here including the use of diblock poly(styrene-*alt*-maleic anhydride) -b- poly(styrene) micelles for solvent mediated PTL sequestration and delivery against the AML cell line MV4-11.[74,75] Furthermore, the enhanced permeability and retention (EPR) effect, which is the preferential uptake and localisation into tumour or infarcted tissues due to the surrounding abnormal vasculature, has been shown to benefit many nanoparticle/drug preparations, which further emphasises a potential advantage of F127 based systems *in vivo* over a co-solvent based formulation.[76,77] Nevertheless, different polymer based coatings can induce different effects. For example, PEGylated lipid nanocapsules have been shown to not impact on human monocytes, whereas Pluronic (F68) coated lipid nanocapsules have been shown to heighten activation of human monocytes but were inert against T-cells, emphasising how polymeric interfaces can modulate cell interactions as well as reducing non-specific binding.[78]

CONCLUSIONS

Solvent-free PTL containing F127 micelles with various peripheral surface charges were synthesised and characterised with respect to their physicochemical behaviour, highlighting the stable incorporation and retention of PTL with thermal reversibility between monomeric and micelle phases. Furthermore, the efficacy of each formulation as a chemotherapeutic delivery agent in the treatment of ALL *in vitro* was demonstrated. Small differences arising from charge-mediated membrane interactions caused changes with their efficacy *in vitro*, with anionic formulations having reduced relative efficacy. However, efficacy was comparable to that of a co-solvent based formulation, highlighting how a solvent-free formulation could be developed as a substitute, thereby removing the requirement for cytotoxic co-solvents in treatments. Moreover, the synthesis of the particles displaying surface bound synthetically accessible groups provides the possibility for the incorporation of additional functionality, for example, increases in cell specificity for the treatment of ALL could be achieved *via* antibody conjugation. In conclusion, the inherent tunability, enhanced retention and improved pharmacokinetics of polymer-based systems in general *in vivo*[62,63,71,72] along with the introduction of peripheral functional groups may enable the future production and delivery of micelle species with improved targeting to the bone marrow niche and maximise the chemotherapeutic potential of PTL.

ASSOCIATED CONTENT

Supporting Information.

Supporting information highlighting additional micelle synthesis (MALDI-TOF, FTIR), characterization (DLS, SAXS, UV-Vis Spectroscopy), uptake (Widefield Microscopy) and activity (Flow Cytometry) data is also available.

AUTHOR INFORMATION

Corresponding Authors

- Adam W. Perriman, School of Cellular and Molecular Medicine, University of Bristol, Bristol, UK. E-mail; chawp@bristol.ac.uk

- Allison Blair. School of Cellular and Molecular Medicine, University of Bristol, Bristol, UK. E-mail; Allison.Blair@bristol.ac.uk

Author Contributions

The manuscript was written through contributions of Robert C. Deller, Paraskevi Diamanti, Allison Blair and Adam W. Perriman. All authors have given approval to the final version of the manuscript.

ACKNOWLEDGMENT

ABBREVIATIONS

PTL, Parthenolide; ALL, acute lymphoblastic leukaemia; hMSC, Human Mesenchymal Stem Cell; AML, acute myeloid leukaemia; CMT, Critical Micelle Concentration; CMT, Critical Micelle Temperature; DLS, Dynamic Light Scattering; SAXS, Small Angle X-ray Scattering; SLS, Static Light Scattering; SLD, Scattering Length Density; PEI, Polyethylenimine; PEG, Polyethylene Glycol; PPG, Polypropylene Glycol; DPH, 1,6-Diphenyl-1,3,5-hexatriene;

REFERENCES

(1)   Savjani, K. T.; Gajjar, A. K.; Savjani, J. K. Drug solubility: importance and enhancement techniques. *ISRN pharmaceutics* **2012**, 1–10 DOI: 10.5402/2012/195727.

(2)   Rautio, J.; Kumpulainen, H.; Heimbach, T.; Oliyai, R.; Oh, D.; Järvinen, T.; Savolainen, J. Prodrugs: design and clinical applications. *Nat Rev Drug Disc* **2008**, *7* (3), 255–270 DOI: 10.1038/nrd2468.

(3)   Shin, H.-C.; Alani, A. W. G.; Rao, D. A.; Rockich, N. C.; Kwon, G. S. Multi-drug loaded polymeric micelles for simultaneous delivery of poorly soluble anticancer drugs. *J Control Release* **2009**, *140* (3), 294–300 DOI: 10.1016/j.jconrel.2009.04.024.

(4)   Schmaljohann, D. Thermo- and pH-responsive polymers in drug delivery. *Adv Drug Deliv Rev* **2006**, *58* (15), 1655–1670 DOI: 10.1016/j.addr.2006.09.020.

(5)   Shamay, Y.; Adar, L.; Ashkenasy, G.; David, A. Light induced drug delivery into cancer cells. *Biomaterials* **2011**, *32*, 1377–1386 DOI: 10.1016/j.biomaterials.2010.10.029.

(6)   Jinqiang Jiang; Xia Tong, A.; Zhao, Y. A New Design for Light-Breakable Polymer Micelles. *Journal of the American Chemical Society* **2005**, *127*, 8290–8291 DOI: 10.1021/ja0521019.

(7)   Broyer, R.; Grover, G.; Maynard, H. D. Emerging synthetic approaches for protein–polymer conjugations. *Chem Comm* **2011**, *47*, 2212–2226 DOI: 10.1039/c0cc04062b.

(8)   Catherine M Goodman; Catherine D McCusker; Tuna Yilmaz, A.; Rotello, V. M. Toxicity of Gold Nanoparticles Functionalized with Cationic and Anionic Side Chains. *Bioconjugate Chem* **2004**, *15*, 897–900 DOI: 10.1021/bc049951i.

(9)   Yuan, Y. Y.; Mao, C. Q.; Du, X. J.; Du, J. Z.; Wang, F.; Wang, J. Surface Charge Switchable Nanoparticles Based on Zwitterionic Polymer for Enhanced Drug Delivery to Tumor. *Adv Mater* **2012**, *24* (40), 5476–5480 DOI: 10.1002/adma.201202296.

(10)   He, C.; Hu, Y.; Yin, L.; Tang, C.; Yin, C. Effects of particle size and surface charge on cellular uptake and biodistribution of polymeric nanoparticles. *Biomaterials* **2010**, *31* (13), 3657–3666 DOI: 10.1016/j.biomaterials.2010.01.065.

(11)   Breunig, M.; Bauer, S.; Göpferich, A. Polymers and nanoparticles: Intelligent tools for intracellular targeting? *Eur J Pharm Sci* **2008**, *68*, 112–128 DOI: 10.1016/j.ejpb.2007.06.010.

(12)   Redaelli, A.; Laskin, B. L.; Stephens, J. M.; Botteman, M. F.; Pashos, C. L. A systematic literature review of the clinical and epidemiological burden of acute lymphoblastic leukaemia (ALL). *Eur J Cancer Care* **2005**, *14* (1), 53–62 DOI: 10.1111/j.1365-2354.2005.00513.x.

(13)   *cancerresearchuk.org*. *http://www.cancerresearchuk.org (accessed December 10, 2015)*.

(14)   Acute Lymphocytic Leukemia - SEER Stat Fact Sheets. *seer.cancer.gov*. *http://seer.cancer.gov/statfacts/html/alyl.html (accessed December 10, 2015)*.

(15)   Inaba, H.; Greaves, M.; Mulligan, C. G. Acute lymphoblastic leukaemia. *Lancet* **2013**, *381* (9881), 1943–1955 DOI: 10.1016/S0140-6736(12)62187-4.

(16)   Vora, A.; Goulden, N.; Mitchell, C.; Hancock, J.; Hough, R.; Rowntree, C.; Moorman, A. V.; Wade, R. Augmented post-remission therapy for a minimal residual disease-defined high-risk subgroup of children and young people with clinical standard-risk and intermediate-risk acute lymphoblastic leukaemia (UKALL 2003): a randomised controlled trial. *Lancet Oncol.* **2014**, *15* (8), 809–818 DOI: 10.1016/S1470-2045(14)70243-8.

(17)   Vora, A.; Goulden, N.; Wade, R.; Mitchell, C.; Hancock, J.; Hough, R.; Rowntree, C.; Richards, S. Treatment reduction for children and young adults with low-risk acute lymphoblastic leukaemia defined by minimal residual disease (UKALL 2003): a randomised controlled trial. *Lancet Oncol.* **2013**, *14* (3), 199–209 DOI: 10.1016/S1470-2045(12)70600-9.

(18)   Hunger, S. P.; Mulligan, C. G. Acute lymphoblastic leukemia in children. *N Engl J Med* **2015**, *373*, 1541–1552 DOI: 10.1056/NEJMra1400972.

(19)   Diamanti, P.; Cox, C. V.; Moppett, J. P.; Blair, A. Parthenolide eliminates leukemia-initiating cell populations and improves survival in xenografts of childhood acute lymphoblastic leukemia. *Blood* **2013**, *121* (8), 1384–1393 DOI: 10.1182/blood-2012-08-448852.

(20)   Prucker, C.; Attarbaschi, A.; Peters, C.; Dworzak, M. N.; Pötschger, U.; Urban, C.; Fink, F.-M.; Meister, B.; Schmitt, K.; Haas, O. A.; et al. Induction death and treatment-related mortality in first remission of children with acute lymphoblastic leukemia: a population-based analysis of the Austrian Berlin-Frankfurt-Münster study group. *Leukemia* **2009**, *23* (7), 1264–1269 DOI: 10.1038/leu.2009.12.

(21)   Wen, J.; You, K. R.; Lee, S. Y.; Song, C. H.; G, K. D. G. Oxidative Stress-mediated Apoptosis. The anticancer effect of the sesquiterpene lactone parthenolide. *J Biol Chem* **2002**, *277* (41), 38954–38964 DOI: 10.1074/jbc.M203842200.

(22)   Guzman, M. L.; Rossi, R. M.; Karnischky, L.; Li, X.; Peterson, D. R.; Howard, D. S.; Jordan, C. T. The sesquiterpene lactone parthenolide induces apoptosis of human acute myelogenous leukemia stem and progenitor cells. *Blood* **2005**, *105* (11), 4163–4169 DOI: 10.1182/blood-2004-10-4135.

(23)   Khadka, P.; Ro, J.; Kim, H.; Kim, I.; Kim, J. T.; Kim, H.; Cho, J. M.; Yun, G.; Lee, J. Pharmaceutical particle technologies: An approach to improve drug solubility, dissolution and bioavailability. *Asian Journal of Pharmaceutical Sciences* **2014**, *9* (6), 304–316 DOI: 10.1016/j.ajps.2014.05.005.

(24)   Guzman, M. L.; Rossi, R. M.; Neelakantan, S.; Li, X.; Corbett, C. A.; Hassane, D. C.; Becker, M. W.; Bennett, J. M.; Sullivan, E.; Lachowicz, J. L.; et al. An orally bioavailable parthenolide analog selectively eradicates acute myelogenous leukemia stem and progenitor cells. *Blood* **2007**, *110* (13), 4427–4435 DOI: 10.1182/blood-2007-05-090621.

(25)   Long, J.; Ding, Y. H.; Wang, P. P.; Zhang, Q.; Chen, Y. Total syntheses and structure–activity relationship study of parthenolide analogues. *Tetrahedron letters* **2016**, *57*, 874–877 DOI: 10.1016/j.tetlet.2016.01.039.

(26)   Alexandridis, P.; Holzwarth, J. F.; Hatton, T. A. Micellization of Poly(ethylene oxide)-Poly(propylene oxide)-Poly(ethylene oxide) Triblock Copolymers in Aqueous Solutions: Thermodynamics of Copolymer Association. *Macromolecules* **1994**, *27* (9), 2414–2425 DOI: 10.1021/ma00087a009.

(27)   Batrakova, E.; Lee, S.; Li, S.; Venne, A.; Alakhov, V.; Kabanov, A. Fundamental Relationships Between the Composition of Pluronic Block Copolymers and Their Hypersensitization Effect in MDR Cancer Cells. *Pharm Res* **1999**, *16* (9), 1373–1379 DOI: 10.1023/A:1018942823676.

(28)   Zhou, Z.; Chu, B. Anomalous micellization behavior and composition heterogeneity of a triblock ABA copolymer of (A) ethylene oxide and (B) propylene oxide in aqueous solution. *Macromolecules* **1988**, *21* (8), 2548–2554 DOI: 10.1021/ma00186a039.

(29)   Alexandridis, P.; Nivaggioli, T.; Hatton, T. A. Temperature Effects on Structural Properties of Pluronic P104 and F108 PEO-PPO-PEO Block Copolymer Solutions. *Langmuir* **1995**, *11*, 1468–1476.

(30)   Collins, A. M.; Zabkiewicz, J.; Ghiggi, C.; Hauser, J. C.; Burnett, A. K.; Mann, S. Tris(8-hydroxyquinolinato)gallium(III)-Loaded Copolymer Micelles as Cytotoxic Nanoconstructs for Cosolvent-Free Organometallic Drug Delivery. *Small* **2011**, *7* (12), 1635–1640 DOI: 10.1002/smll.201100405.

(31)   Zhang, W.; Shi, Y.; Chen, Y.; Ye, J.; Sha, X.; Fang, X. Multifunctional Pluronic P123/F127 mixed polymeric micelles loaded with paclitaxel for the treatment of multidrug resistant tumors. *Biomaterials* **2011**, *32*, 2894–2906 DOI: 10.1016/j.biomaterials.2010.12.039.

(32)   Zhang, W.; Shi, Y.; Chen, Y.; Yu, S.; Hao, J.; Luo, J.; Sha, X.; Fang, X. Enhanced antitumor

efficacy by Paclitaxel-loaded Pluronic P123/F127 mixed micelles against non-small cell lung cancer based on passive tumor targeting and modulation of drug resistance. *Eur J Pharm Biopharm* **2010**, *75* (3), 341–353 DOI: 10.1016/j.ejpb.2010.04.017.

(33)   Zhang, W.; Gilstrap, K.; Wu, L.; K C, R. B.; Moss, M. A.; Wang, Q.; Lu, X.; He, X. Synthesis and characterization of thermally responsive Pluronic F127-chitosan nanocapsules for controlled release and intracellular delivery of small molecules. *ACS Nano* **2010**, *4* (11), 6747–6759 DOI: 10.1021/nn101617n.

(34)   Liu, T.; Zhang, X.; Ke, B.; Wang, Y.; Wu, X.; Jiang, G.; Wu, T.; Nie, G. F-127-PEI co-delivering docetaxel and TFPI-2 plasmid for nasopharyngeal cancer therapy. *Mater Sci Eng C Mater Biol Appl* **2016**, *61*, 269–277 DOI: 10.1016/j.msec.2015.12.049.

(35)   Bogomolova, A.; Hruby, M.; Panek, J.; Rabyk, M.; Turner, S.; Bals, S.; Steinhart, M.; Zhigunov, A.; Sedlacek, O.; Stepanek, P.; et al. Small-angle X-ray scattering and light scattering study of hybrid nanoparticles composed of thermoresponsive triblock copolymer F127 and thermoresponsive statistical polyoxazolines with hydrophobic moieties. *J Appl Crystallogr* **2013**, *46* (6), 1690–1698 DOI: 10.1107/S0021889813027064.

(36)   Sehgal, D.; Vijay, I. K. A Method for the High Efficiency of Water-Soluble Carbodiimide-Mediated Amidation. *Anal Biochem* **1994**, *218* (1), 87–91 DOI: 10.1006/abio.1994.1144.

(37)   Strohalm, M.; Hassman, M.; Košata, B.; Kodíček, M. mMass data miner: an open source alternative for mass spectrometric data analysis. *Rapid Communications in Mass Spectrometry* **2008**, *22* (6), 905–908 DOI: 10.1002/rcm.3444.

(38)   FDA F127 Approval. *accessdata.fda.gov*.

(39)   Axelsson, J.; Scrivener, E.; Haddleton, D. M.; Derrick, P. J. Mass Discrimination Effects in an Ion Detector and Other Causes for Shifts in Polymer Mass Distributions Measured by Matrix-Assisted Laser Desorption/Ionization Time-of-Flight Mass Spectrometry. *Macromolecules* **1996**, *29*, 8875–8882.

(40)   Zhang, X.; Jackson, J.; M, B. H. Determination of surfactant critical micelle concentration by a novel fluorescence depolarization technique. *J Biochem Biophys Methods* **1996**, *31*, 145–150.

(41)   Wanka, G.; Hoffmann, H.; Ulbricht, W. Phase Diagrams and Aggregation Behavior of Poly(oxyethylene)-Poly(oxypropylene)-Poly(oxyethylene) Triblock Copolymers in Aqueous Solutions. *Macromolecules* **1994**, *27* (15), 4145–4159 DOI: 10.1021/ma00093a016.

(42)   Alexandridis, P.; Hatton, T. A. Poly(ethylene oxide)-poly(propylene oxide)-poly(ethylene oxide) block copolymer surfactants in aqueous solutions and at interfaces: thermodynamics, structure, dynamics, and modeling. *Colloids and Surfaces A: Physicochemical and Engineering Aspects* **1995**, *96*, 1–46.

(43)   Hvidt, S.; Batsberg, W. Characterization and Micellization of a Poloxamer Block Copolymer. *International Journal of Polymer Analysis and Characterization* **2007**, *12* (1), 13–22 DOI: 10.1080/10236660601094093.

(44)   Zhang, C.; Wu, F.-G.; Hu, P.; Chen, Z. Interaction of Polyethylenimine with Model Cell Membranes Studied by Linear and Nonlinear Spectroscopic Techniques. *J. Phys. Chem. C* **2014**, *118* (23), 12195–12205 DOI: 10.1021/jp502383u.

(45)   Kircheis, R.; Schüller, S.; Brunner, S. Polycation-based DNA complexes for tumor-targeted gene delivery in vivo - Kircheis - 1999 - The Journal of Gene Medicine - Wiley Online Library. *The journal of gene …* **1999**.

(46)   Wilkins, L. E.; Phillips, D. J.; Deller, R.; Davies, G.-L.; Gibson, M. I. Synthesis and characterisation of glucose-functional glycopolymers and gold nanoparticles: study of their potential interactions with ovine red blood cells. *Carbohydr Res* **2015**, *405*, 47–54 DOI: 10.1016/j.carres.2014.09.009.

(47)   Lee, S. H.; Choi, S. H.; Kim, S. H.; Park, T. G. Thermally sensitive cationic polymer

nanocapsules for specific cytosolic delivery and efficient gene silencing of siRNA: Swelling induced physical disruption of endosome by cold shock. *J Control Release* **2008**, *125*, 25–32.

(48) Fischer, D.; Li, Y.; Ahlemeyer, B.; Krieglstein, J. In vitro cytotoxicity testing of polycations: influence of polymer structure on cell viability and hemolysis. *Biomaterials* **2003**, *24*, 1121–1131.

(49) Lunov, O.; Syrovets, T.; Loos, C.; Beil, J.; Delacher, M.; Tron, K.; Nienhaus, G. U.; Musyanovych, A.; Mailänder, V.; Landfester, K.; et al. Differential uptake of functionalized polystyrene nanoparticles by human macrophages and a monocytic cell line. *ACS Nano* **2011**, *5* (3), 1657–1669 DOI: 10.1021/nn2000756.

(50) Uccelli, A.; Moretta, L.; Pistoia, V. Mesenchymal stem cells in health and disease. *Nat Rev Immunol* **2008**, *8* (9), 726–736 DOI: 10.1038/nri2395.

(51) Arranja, A.; Schroder, A. P.; Schmutz, M.; Waton, G. Cytotoxicity and internalization of Pluronic micelles stabilized by core cross-linking. *J Control Release* **2014**, *196*, 87–95.

(52) Steele, A. J.; Jones, D. T.; Ganeshaguru, K.; Duke, V. M.; Yogashangary, B. C.; North, J. M.; Lowdell, M. W.; Kottaridis, P. D.; Mehta, A. B.; Prentice, A. G.; et al. The sesquiterpene lactone parthenolide induces selective apoptosis of B-chronic lymphocytic leukemia cells in vitro. *Leukemia* **2006**, *20* (6), 1073–1079 DOI: 10.1038/sj.leu.2404230.

(53) O'Brien, J.; Wilson, I.; Orton, T.; Pognan, F. Investigation of the Alamar Blue (resazurin) fluorescent dye for the assessment of mammalian cell cytotoxicity. *Eur J Biochem* **2000**, *267* (17), 5421–5426.

(54) Arranja, A.; Denkova, A. G.; Morawska, K.; Waton, G.; van Vlierberghe, S.; Dubruel, P.; Schosseler, F.; Mendes, E. Interactions of Pluronic nanocarriers with 2D and 3D cell cultures: Effects of PEO block length and aggregation state. *J Control Release* **2016**, *224*, 126–135 DOI: 10.1016/j.jconrel.2016.01.014.

(55) Palte, M. J.; Raines, R. T. Interaction of Nucleic Acids with the Glycocalyx. *Journal of the American Chemical Society* **2012**, *134*, 6218–6223 DOI: 10.1021/ja2106477.

(56) Fuchs, S. M.; Raines, R. T. Arginine Grafting to Endow Cell Permeability. *ACS Chemical Biology* **2007**, *2*, 167–170.

(57) Johnson, R. J.; Chao, T. Y.; Lavis, L. D.; Raines, R. T. Cytotoxic Ribonucleases: The Dichotomy of Coulombic Forces†. *Biochemistry* **2007**, *46*, 10308–10316 DOI: 10.1021/bi700857u.

(58) Futami, J.; Kitazoe, M.; Murata, H.; Yamada, H. Exploiting protein cationization techniques in future drug development. *Expert Opin. Drug Discov.* **2007**, *2* (2), 261–269 DOI: 10.1517/17460441.2.2.261.

(59) Van Vlierberghe, P.; Ferrando, A. The molecular basis of T cell acute lymphoblastic leukemia. *J. Clin. Invest.* **2012**, *122* (10), 3398–3406 DOI: 10.1172/JCI61269.

(60) Vermes, I.; Haanen, C.; Steffens-Nakken, H.; Reutellingsperger, C. A novel assay for apoptosis Flow cytometric detection of phosphatidylserine expression on early apoptotic cells using fluorescein labelled Annexin V. *J Immunol Methods* **1995**, *184* (1), 39–51 DOI: 10.1016/0022-1759(95)00072-I.

(61) Yang, Z.-J.; Ge, W.-Z.; Li, Q.-Y.; Lu, Y.; Gong, J.-M.; Kuang, B.-J.; Xi, X.; Wu, H.; Zhang, Q.; Chen, Y. Syntheses and Biological Evaluation of Costunolide, Parthenolide, and Their Fluorinated Analogues. *J Med Chem* **2015**, *58* (17), 7007–7020 DOI: 10.1021/acs.jmedchem.5b00915.

(62) Mu, C. F.; Balakrishnan, P.; Cui, F. D.; Yin, Y. M.; Lee, Y. B. The effects of mixed MPEG–PLA/Pluronic® copolymer micelles on the bioavailability and multidrug resistance of docetaxel. *Biomaterials* **2010**, *31*, 2371–2379 DOI: 10.1016/j.biomaterials.2009.11.102.

(63) Xiao, K.; Li, Y.; Luo, J.; Lee, J. S.; Xiao, W.; Gonik, A. M.; Agarwal, R. G.; Lam, K. S. The

effect of surface charge on in vivo biodistribution of PEG-oligocholic acid based micellar nanoparticles. *Biomaterials* **2011**, *32* (13), 3435–3446 DOI: 10.1016/j.biomaterials.2011.01.021.

(64)   Cedervall, T.; Lynch, I.; Lindman, S.; Berggård, T.; Thulin, E.; Nilsson, H.; Dawson, K. A.; Linse, S. Understanding the nanoparticle-protein corona using methods to quantify exchange rates and affinities of proteins for nanoparticles. *Proc Natl Acad Sci USA* **2007**, *104* (7), 2050–2055 DOI: 10.1073/pnas.0608582104.

(65)   Tenzer, S.; Docter, D.; Kuharev, J.; Musyanovych, A.; Fetz, V.; Hecht, R.; Schlenk, F.; Fischer, D.; Kiouptsi, K.; Reinhardt, C.; et al. Rapid formation of plasma protein corona critically affects nanoparticle pathophysiology. *Nature Nanotech* **2013**, *8* (10), 772–781 DOI: 10.1038/nnano.2013.181.

(66)   Walkey, C. D.; Olsen, J. B.; Song, F.; Liu, R.; Guo, H.; Olsen, D. W. H.; Cohen, Y.; Emili, A.; Chan, W. C. W. Protein Corona Fingerprinting Predicts the Cellular Interaction of Gold and Silver Nanoparticles. *ACS Nano* **2014**, *8*, 2439–2455 DOI: 10.1021/nn406018q.

(67)   Wei, Q.; Becherer, T.; Angioletti-Uberti, S.; Dzubiella, J.; Wischke, C.; Neffe, A. T.; Lendlein, A.; Ballauff, M.; Haag, R. Protein Interactions with Polymer Coatings and Biomaterials. *Angew Chem Int Edit* **2014**, No. 53, 8004–8031 DOI: 10.1002/anie.201400546.

(68)   Schöttler, S.; Becker, G.; Winzen, S.; Steinbach, T.; Mohr, K.; Landfester, K.; Mailänder, V.; Wurm, F. R. Protein adsorption is required for stealth effect of poly(ethylene glycol)- and poly(phosphoester)-coated nanocarriers. *Nature Nanotech* **2016**, *11* (4), 372–377 DOI: 10.1038/nnano.2015.330.

(69)   Alconcel, S.; Baas, A.; Maynard, H. D. FDA-approved poly (ethylene glycol)–protein conjugate drugs. *Polym Chem* **2011**, *2*, 1442–1448 DOI: 10.1039/c1py00034a.

(70)   Otsuka, H.; Nagasaki, Y.; Kataoka, K. PEGylated nanoparticles for biological and pharmaceutical applications. *Adv Drug Deliv Rev* **2003**, *55* (3), 403–419.

(71)   Tan, J. S.; Butterfield, D. E.; Voycheck, C. L.; Caldwell, K. D.; Li, J. T. Surface modification of nanoparticles by PEO/PPO block copolymers to minimize interactions with blood components and prolong blood circulation in rats. *Biomaterials* **1993**, *14* (11), 823–833.

(72)   Dunn, S. E.; Coombes, A.; Garnett, M. C.; Davis, S. S. In vitro cell interaction and in vivo biodistribution of poly(lactide-co-glycolide) nanospheres surface modified by poloxamer and poloxamine copolymers. *J Control Release* **1997**, *44*, 65–76.

(73)   Stolnik, S.; Daudali, B.; Arien, A.; Whetstone, J.; Heald, C. R.; Garnett, M. C.; Davis, S. S.; Illum, L. The effect of surface coverage and conformation of poly(ethylene oxide) (PEO) chains of poloxamer 407 on the biological fate of model colloidal drug carriers. *Biochimica et Biophysica Acta (BBA)* **2001**, *1514* (2), 261–279.

(74)   Kwon, G. S.; Forrest, M. L. Amphiphilic block copolymer micelles for nanoscale drug delivery. *Drug Dev. Res.* **2006**, *67* (1), 15–22 DOI: 10.1002/ddr.20063.

(75)   Baranello, M. P.; Bauer, L.; Jordan, C. T.; Benoit, D. S. W. Micelle Delivery of Parthenolide to Acute Myeloid Leukemia Cells. *Cel. Mol. Bioeng.* **2015**, *8* (3), 455–470 DOI: 10.1007/s12195-015-0391-x.

(76)   Kwon, G.; Suwa, S.; Yokoyama, M.; Okano, T.; Sakurai, Y.; Kataoka, K. Enhanced tumor accumulation and prolonged circulation times of micelle-forming poly (ethylene oxide-aspartate) block copolymer-adriamycin conjugates. *J Control Release* **1994**, *29* (1-2), 17–23 DOI: 10.1016/0168-3659(94)90118-X.

(77)   Torchilin, V. Tumor delivery of macromolecular drugs based on the EPR effect. *Adv Drug Deliv Rev* **2011**, *63* (3), 131–135 DOI: 10.1016/j.addr.2010.03.011.

(78)   Farace, C.; Sánchez-Moreno, P.; Orecchioni, M.; Manetti, R.; Sgarrella, F.; Asara, Y.; Peula-García, J. M.; Marchal, J. A.; Madeddu, R.; Delogu, L. G. Immune cell impact of three

differently coated lipid nanocapsules: pluronic, chitosan and polyethylene glycol. *Scientific Reports* **2016**, *6*, 18423 DOI: 10.1038/srep18423.

TABLE OF CONTENTS GRAPHIC